Journal of Photochemistry, 9 (1978) 341 - 361

PHOTOCHEMICAL CONCENTRATION MODULATION AND ITS APPLICATION TO THE DETECTION OF LOW CONCENTRATION PHOTOCHEMICAL POLLUTANTS IN THE AIR

CHIA-LUN J. HU

Department of Electrical Engineering, University of Colorado, Boulder, Colo. 80309 (U.S.A.)

(Received November 10, 1977)

Summary

Conventional spectroscopic methods of detection of low concentration pollutants in the air generally suffer from severe optical noise as well as electronic noise. This optical noise usually includes characteristic overlapping noise, background radiation noise and d.c. beam fluctuation noise and in many cases is difficult to eliminate using conventional methods. However, because most photosensitive pollutants will decompose into other chemical species under UV illumination at a specific wavelength, we can vary the concentrations of these pollutants by controlling the intensity of the UV beam while keeping the optical noise unchanged. Thus, by using this intensity-controlled UV beam, we can create a controlled difference between the signal and the noise. Several techniques can then be used to detect this modulated signal in the presence of the unmodulated noise. We shall report two approaches for measuring the concentrations of pollutants following this concept of concentration modulation. One entails shifting the monitored line position to a high absorption, low noise region of the spectrum by observing the products produced by concentration modulation. The other uses modern communication engineering technology to extract the weak modulated signal from the noise. Experimental results of the first approach using NO_2 as an example are reported in detail. The results verify both qualitatively and quantitatively the basic concept of concentration modulation and show an improvement in sensitivity such that 0.5 ppm NO_2 is measurable using this method. This sensitivity may be difficult to reach with conventional spectroscopic methods using the same path length.

1. Introduction — background survey

Since this paper reports a novel approach† to the sensitive spectroscopic detection of air pollutants by means of applying flash modulation to

†Patent application of the ideas and schemes reported in this paper is pending.

the concentration of pollutants, it is logical to survey the background studies in both flash spectroscopic techniques and spectroscopic detection of air pollutants. Porter and West [1] published in 1974 an excellent review article on the techniques of flash photolysis in which 213 references were cited. They reviewed various types of instrumentation for flash spectroscopy, kinetic spectrometry, and nanosecond and picosecond flash techniques (or Q-switched and mode-locked lasers). As well as these topics methods for monitoring or analyzing the transient products, which are of most interest to the present paper as far as the background survey is concerned, were also discussed in detail. These methods include various spectrometric methods such as absorption, fluorescence, IR, electron spin resonance (ESR), nuclear magnetic resonance (NMR) and mass spectrometry. Electrochemical methods are occasionally used for liquid samples with high conductivities. The absorption spectrometric method is the most commonly used of all these methods and will be discussed later in some detail with reference to recent developments. The fluorescence method of monitoring has the advantage of eliminating the d.c. beam noise by monitoring the fluorescence emissions from the sides. Also if a super-narrow flashing pulse (*e.g.* the pulse produced by a mode-locked UV laser) is used to obtain an excited state with a long lifetime, one can resolve the fluorescent emission from the flash in the time domain by electronic gating techniques. IR monitoring of flash products has become quite popular in the last ten years with the development of sensitive fast responding low temperature solid state IR detectors such as germanium:copper detectors, InSb detectors etc. It should be noted that the monitoring light in IR spectrometry is easier to separate from the UV flash than the visible monitoring light. Mass spectrometry (mostly time-of-flight type) requires expensive and bulky equipment and has been used on NO_2, tetramethyl-lead, $Fe(CO)_5$–NO mixtures and other hydrocarbon flash photolysis studies. ESR and NMR spectrometry are mostly restricted to the detection of those products (mostly radicals) having significantly different ESR and NMR spectra than those of the unflashed species. Finally, electrochemical methods utilize some differential electrolysis and photovoltaic effects in certain conducting liquids to detect the chemical changes generated by the flash in these liquids. Recent studies of flash photolysis effects have mostly concentrated on biological and organic materials such as tryptophan, tyrosine [2], lysozyme [3], duroquinone [4], rhodamine derivatives [5], vinyl monomers [6] etc.

Of all these monitoring systems, absorption spectrometry is still the most common method for monitoring the photochemical changes of inorganic gases under flash photolysis. This was also the classical method developed by Porter [7] in 1950. Recent studies of this method include such modifications as modulated double-beam null detection [8], signal-averaging detection [9] and spectrophone detection [10]. The modulated double-beam detection method utilizes two monitoring beams split from an amplitude-modulated source, one going through a blank cell and the other through a sampling cell. The outputs of these two beams detected by two

photomultipliers are fed into two phase-locked amplifiers which eliminate most of the electronic noise and then into a difference amplifier. The output of the difference amplifier then gives a net change due to the flash photolysis in the sampling cell. The signal-averaging scheme uses repetitive flashes and it converts the analogue signal generated by each flash into a digital signal such that it can be cumulatively stored in a digital memory. The random noise associated with the signals is therefore averaged out while the signals themselves are added cumulatively. This process is different from the one discussed here in that it does not use the correlation property of the output beam immediately before and immediately after each flash. This will be discussed in detail in Section 5. The spectrophone monitoring method employs the effect that when most gases are photolyzed the volume expands because of the increase in the number of molecules, or the release of heat due to photochemical reactions or both. Therefore, a microphone-type detector can be used to detect this acoustic expansion strength very sensitively, and from the electrical response of the microphone quantitative measurement of the degree of photolysis may be recorded. This method has the advantage that the microphone will only respond to a net sudden change and not to the d.c. drift or slow fluctuation of the gas volume. Thus it does not suffer from d.c. beam noise as is the case in conventional absorption spectrometry. The disadvantage is, however, that it is difficult to identify or to differentiate the photolyzed species and photochemical reactions by this method alone. Finally, Johnson *et al.* [11] at Berkeley in 1967 attempted a scheme using a conventional (or radio engineering) frequency shift and filtering technique for detecting the absorption line of a pollutant which is continuously flash modulated. Some qualitative phase measurements were reported using this method in spite of the existence of several very doubtful design approaches.

As to the spectrometric detection of air pollutants, a review of the current methods shows that it can be approximately divided into two major groups: *in situ* measurements and remote-sensing schemes. Stern has edited an excellent series of books on various subjects of air pollutants. The most recent edition of this series [12] contains five volumes with Volume III specially devoted to measuring, monitoring and surveillance of air pollutants. This volume reviews most of the schemes contained in both of the two groups just mentioned. The first group includes mainly the spectrometric methods using long-path absorptions, fluorescence, flame photometry, chemiluminescence and mass analysis. The 430 m long-path IR gas cell at the Franklin Institute has been used to analyze the polluted atmosphere down to 100 ppb levels [13]. A 250 ft long-path UV spectrometer has also been used to measure the local ozone concentration in air [14]. Hanst has surveyed a number of IR lasers which are of potential use in the absorption spectroscopic detection of pollutants [15], and many tunable dye lasers have been used in pollutant absorption spectrometry [16]. The fluorescence spectrometric method has the advantage of avoiding d.c. optical noise and has been used in the detection of H_2S [17, 18], NO_2 [19,

20], chlorophyll, phenol, sulfonates and rhodamine W.T. [21]. Flame photometry is mainly used to detect phosphorus and sulfur compounds [22, 23]. When these substances are burned in a hydrogen flame, characteristic emission lines of sulphur and phosphorus can be detected spectroscopically. The chemiluminescent technique employs the characteristic emission of light generated from chemical reactions such as NO_2 + ozone or ozone + rhodamine B [24, 25]. Therefore if these characteristic emissions are measured in a dark chamber with saturated ozone or NO_2, a quantitative measurement is obtained of the other species involved. Mass spectrometry utilizes high energy electron impact on the polluted air sample such that the pollutant molecules are ionized and differentiated by different flight paths under a magnetic field. Alternatively, these ions can also be differentiated by d.c. electric field acceleration such that ions with different masses attain different velocities. Therefore they will take different times of flight to reach the collecting electrode. Consequently resolving the current pulses in time at the collecting electrode will not only give us the identities of these ions but also the proportional amounts of the ions. Hence the original pollutant species can be identified and quantitatively measured. A complete review of the application of mass spectrometry to environmental measurements is given by Alford's article published in 1977 which includes 272 references [26].

The major remote-sensing techniques include the laser heterodyne receiver, Raman and fluorescent scattering, lidar and elastic scattering, interferometry and correlation spectrometry. The laser heterodyne method [27, 28] employs the well-known radio engineering technology of beating the weak incoming laser-backscattered signal with a local oscillator (laser) signal such that the signal-to-noise ratio of detection can be much enhanced. The Raman [29, 30] and fluorescent scattering [31] of pollutant molecules excited by a UV high power laser with arbitrary wavelength (for Raman scattering) and with resonant wavelength (for fluorescent scattering) will carry characteristic spectra of the pollutants. Therefore by detecting these backscattered emissions with a high resolution spectrometer one can obtain a quantitative measurement on the concentration of remotely located pollutants. Also by measuring the round-trip traveling time of the light pulse by an electronic gating technique (used in radar) one can calculate the range of the polluted area. Parallel to these Raman and fluorescent methods, a variety of lidar systems [32] have been developed using high power pulsed lasers to detect the elastic scattering† from particulate matter or aerosols located remotely.

Interference spectrometry [33 - 35] is a technique using Michelson's interferometer with one reflecting mirror moving at a constant speed. The combined output beam will thus have an intensity which has a time variation proportional to the Fourier transform of the frequency spectrum of the

†Many investigators prefer to use the term "lidar" to include both elastic and inelastic (Raman, fluorescent etc.) scattering.

original light beam [33]. If an on-line computer is used which applies an inverse Fourier transform to the combined beam, the original frequency spectrum can be constructed on-line and hence the remote source emitting light into this device can be analyzed. This method has the advantage over the conventional spectrometry methods in that the whole incident beam, rather than a dispersed portion of it, is used to construct the frequency spectrum. Therefore a higher signal-to-noise ratio has been obtained using this method. This method has been used successfully in the NASA Viking project for remote detection of CO_2 concentration in the Martian atmosphere. Finally, correlation spectrometry [36 - 38] has been used in many remote detection processes. It uses a vibrating mask at the output of a prism-dispersed or grating-dispersed beam. The opening lines of the mask match the absorption spectrum of a particular pollutant. Therefore there is one position during the vibration at which the mask is perfectly correlated with the dispersed beam for that pollutant while no such correlation exists for any other pollutant species. Consequently, selective detection of a particular pollutant from noise is possible.

Apart from all the schemes discussed above, this article reports a novel approach which is directed towards the increase of the signal-to-noise ratio over optical noise. Section 2 is devoted to a general discussion of optical noise and its effect on the spectrometric detection of trace chemicals.

2. Optical noise in the spectroscopic detection of low concentrations of gases

When a trace substance in air (*e.g.* the air pollutants NO_2, SO_2, NH_3 etc.) is to be determined quantitatively using spectroscopic methods the signal is usually very weak and masked by noise. In general, there are two major types of noise: electronic noise and optical noise. The electronic noise is generated in the photodetector and amplifier circuits. It can generally be filtered out using a low-pass filter or it can be relatively reduced if the optical signal is increased. (The optical signal can be increased by, for example, increasing the absorption path in the absorption cell or broadening the absorption linewidth using pressure-broadening techniques etc.) The optical noise, however, is very difficult to remove. This noise usually consists of three major sources: (1) overlapping of the absorption or emission lines of major atmospheric molecules (O_2, N_2, H_2O, CO_2 etc.) with those of the gaseous molecules under investigation; (2) background radiation; (3) fluctuation of the d.c. level of the absorbed light in absorption spectrometry.

The overlapping noise is proportionally increased when one tries to increase the optical signal by, for example, increasing the absorption path, and it cannot be eliminated by chopping the beam. The common air pollutants NO_2 and SO_2 are taken as examples. The strongest absorption lines of NO_2 and SO_2 are at 6.3 μm and 7.35 μm respectively in the IR. These lines are partly or completely masked by the absorption lines of water vapor in the atmosphere. Any attempt to enhance the optical signal by increasing

the absorption path or the absorption linewidth is useless because the absorption of H_2O along the optical path is proportionally increased and still masks the signal. The same applies if one wishes to detect the thermal emission lines of these species in a remote-detection scheme, because by Kirchhoff's radiation law a strong absorption line is usually associated with a strong emission line at the same wavelength. Therefore the strongest thermal emission lines of NO_2 and SO_2 are still at 6.3 μm and 7.35 μm respectively and consequently are still seriously masked by the absorption of water vapor in the air.

The second type of optical noise, the background radiation, is more important in remote-detection schemes than in *in situ* absorption spectrometry. This noise includes sunlight, thermal emission from the sky and clouds (or other background objects), scattering by particulate matter in the air, thermal emission from the walls of the sampling cell for an *in situ* absorption scheme etc. The average of this optical noise has a more or less continuous black body emission spectrum. It will also mask the signal and cannot be eliminated by chopping the incident beam for the case of remote detection.

The third noise source, d.c. fluctuation, exists only in absorption schemes. Because the absorption is weak, any fluctuation of the transmitted optical beam (due to an unstable light source, warm-up effect in the light source, thermal turbulence, mechanical vibration in the absorption chamber etc.) will obscure the signal to be detected. This d.c. optical fluctuation noise can be reduced to some extent by using a folded absorption path. When the number of folds increases, however, the stability of the optical alignment, the light beam inhomogeneity etc. will impose another set of d.c. fluctuation problems which may eventually negate the gain due to path folding.

All these types of optical noise can, however, be efficiently eliminated or diverted if one can apply concentration modulation to the species under detection. This is the main subject to be discussed in Section 3.

3. Concentration modulation

If a gas, *e.g.* NO_2, which exists in low concentrations in air is photosensitive[†], *i.e.* if it can be dissociated into other chemical species under the illumination of a specific UV beam with $\lambda_{UV} < \lambda_{dissociation}$[††], then we can modulate the concentration of this gas by varying the intensity of the UV beam while leaving all the optical noise unchanged. Two different ap-

[†] The pollutants NO_2, SO_2, O_3, NH_3, etc. are all photosensitive. Consequently, the name "photochemical" pollutants is frequently used for these species.

[††] Sometimes when λ_{UV} is greater than λ_{diss}, the pollutant molecules may be excited to higher energy states and react with other molecules in air to form stable products. This will also serve the same purpose of concentration modulation.

proaches can then be followed to measure sensitively the concentration of the gas in the noisy environment.

3.1. Shifting the detection to a stronger absorption region after concentration modulation

In many cases the photolyzed products produced by this UV illumination may have much stronger absorption lines than those of the original species. For example, ozone obtained by photolyzing NO_2 in air has $\alpha(O_3) = 3250\ l\ mol^{-1}\ cm^{-1}$ at 2550 Å which is 15 - 20 times higher than any $\alpha(NO_2)$ in the whole spectrum from IR to UV. Therefore, if we use a monochromator to monitor one of the strong lines produced by the products, we can measure much more sensitively the concentration change due to this concentration modulation. From this we can calculate the concentration of the original species accurately. Using this method the optical noise discussed in Section 1 in general can be either avoided or significantly reduced. For example, the 2550 Å ozone line discussed previously is not in the characteristic absorption regions of any major atmospheric constituents, and hence the overlapping noise is much less serious here than it is at the strongest NO_2 line which is at 6.3 μm in the IR. The background radiation noise should also be much smaller at 2550 Å than it is in the IR and visible regions because, to a rough approximation, the average background radiation as calculated by the black body radiation formula at 300 K will decrease steadily from IR to UV[†]. Furthermore, the d.c. fluctuation noise can be significantly reduced as can be seen from the following example. When the absorption is weak, the low frequency fluctuation and the d.c. drift of the intensity of the light source used in the absorption spectrometry will become important. They may mask completely the change of light intensity due to sample absorption as shown in Fig. 1(a). However, with concentration modulation the monochromator output intensity is subject to a step change Δ at the time when the UV photolyzing pulse is applied as shown in Fig. 1(b). Although comparable with the fluctuation noise, Δ can easily be differentiated from the noise and is readily measurable (see Section 4). Using this step change the concentration of the original species can be accurately calculated as is shown in Section 4.

Consequently, it is seen that by using this wavelength-shifting method we can not only increase the optical signal but also reduce the optical noise significantly.

3.2. Applying signal processing to detect the concentration-modulated signal

If we apply a continuously pulsed UV beam to the polluted air sample, the concentration of a specific photosensitive pollutant, *e.g.* NO_2, will undergo a step decrease Δ at each pulse as shown in Fig. 2. Now, because of this concentration change the intensity of the characteristic emission (or

[†]By Wien's displacement law, the maximum radiation wavelength for a black body at 300 K is 2897/300 or 9.37 μm.

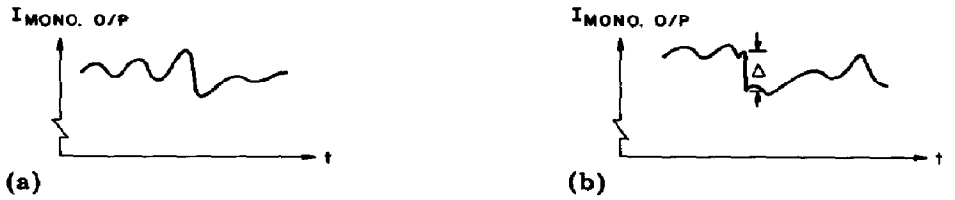

Fig. 1. (a) Monochromator output without concentration modulation; the absorption is masked by the fluctuation and drift of the light source. (b) Monochromator output with concentration modulation; the modulated step change Δ is detectable from the noise.

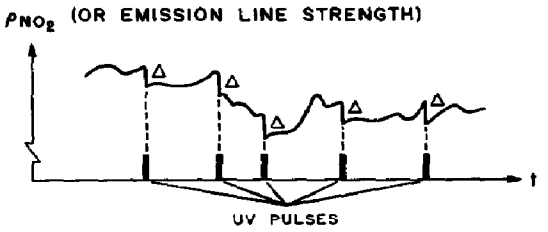

Fig. 2. Concentration modulation using continuous UV pulses.

absorption) line at the monochromator output will also follow the same (or inverse) variation in time, and the Δs in this output will carry the information of the original concentration of the pollutant (Section 4). Although it is non-periodic and still masked by noise, this Δ is a controlled change at a set of pre-ordained times. Consequently, signal processing or communication engineering techniques can be applied to detect sensitively this modulated signal from the unmodulated noise (optical noise). This is the main subject discussed in Section 4.

The types of optical noise discussed in Section 1 are partially shown by the fluctuation of the curve in Fig. 2. These types of noise are not affected by UV modulation and hence they can largely be eliminated after signal processing as explained in detail in Section 5.

The two schemes discussed above can of course be combined to make use of the advantages of both, *i.e.* if we apply signal processing to the monitored output at a strong emission or absorption line of a product coming out of the concentration modulation we may push the signal-to-noise ratio beyond the values obtained from individual schemes. It is now seen that the main aim of concentration modulation is to create some controllable differences between the signal and the optical noise such that either the signal can be shifted out of the noise region, or some communication engineering techniques can be applied to detect this modulated signal from the unmodulated noise or both methods can be used.

As far as the instrumentation is concerned, the technique to be used in concentration modulation is very similar to that used in flash spectroscopy except that it is used in a quite different way. Flash spectroscopy generally uses a strong UV flashing pulse to photolyze photosensitive chemicals in an

absorption cell and to monitor the characteristic lines of any intermediate species immediately after the flash. This technique is mainly used to identify the short-life intermediates appearing after the flash. The lifetimes of these intermediates may be milliseconds or less, but their concentrations are generally very high. Therefore its main requirement is usually an accurate electronic timing circuit to measure the characteristic absorption line intensity at a very short but accurate time after the flash. From these data the identities, the quantum yields and the lifetimes of the intermediates may be determined accurately. In our experiments, however, we are using similar techniques to measure the concentrations of trace gases in polluted air. The lifetimes of the products after photolysis, *e.g.* NO and ozone produced by flashing NO_2 in air, may be very long if the concentrations of the original gases (pollutants) are very low, *e.g.* 1 - 10 ppm†. Therefore in our experiments we are primarily concerned with detection of a weak signal masked by noise so that accurate measurements on the concentrations of the pollutants are possible. We are not particularly interested in the lifetimes or quantum yields of the intermediates immediately after the flash. Therefore the electronic detection system used here will be quite different from those used in flash spectrometry.

4. Wavelength-shifting method in concentration modulation

To verify the advantages of the first method discussed in the former section, we have built a single-flash high intensity modulating system for detecting the low concentration NO_2 in air. The high intensity UV pulse we used allows us to have a deep or saturated modulation on the NO_2 concentration. Consequently, we can already measure the NO_2 concentration in air sensitively without signal processing. This method is based on the following.

When a strong UV flashing pulse is applied to a polluted air sample in the absorption chamber, NO_2 undergoes the following well-known photochemical reactions [39 - 41]:

$$NO_2 \xrightarrow[h\nu(\text{flash})]{k} NO + O \qquad \text{(almost instantaneous)} \qquad (1)$$

$$O + O_2 + M \longrightarrow O_3 + M \qquad \text{(about 40 } \mu\text{s)}^{\dagger\dagger} \qquad (2)$$

---

†The lifetime of a product produced by photolysis depends on the speed of the recovery reaction (which returns the product to the original species). This rate of recovery is proportional to the concentration of the product which is, in turn, proportional to the concentration of the original species undergoing flash photolysis. Therefore the lower the original pollutant concentration the longer are the lives of the photolyzed products (see for example the analysis of the lifetimes of NO and ozone in Appendix 2).

††From ref. 42 (Table 35, p. 119),

$$\tau = \frac{1}{(k_3[O_3][M])_{25\,^\circ C}} = \frac{1}{2.4 \times 10^4} = 40\ \mu s.$$

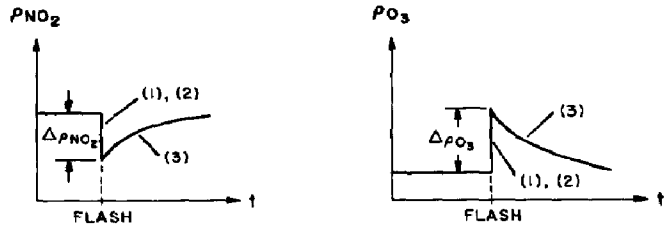

Fig. 3. NO_2 concentration modulation.

Fig. 4. Ozone concentration modulation.

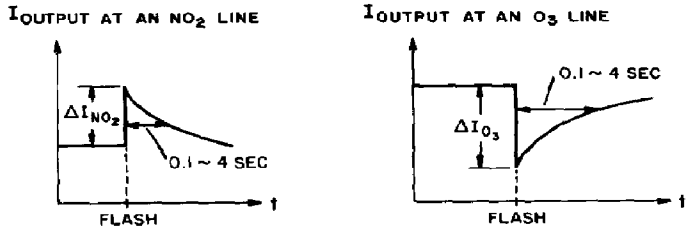

Fig. 5. Monochromator output at an NO_2 line.

Fig. 6. Monochromator output at an ozone line.

$$O_3 + NO \longrightarrow NO_2 + O_2 \qquad \text{(about 0.1 - 4 s)}^{\dagger} \qquad (3)$$

The first two reactions are the modulation reactions (NO_2 decreases and ozone increases). The third reaction is the recovery reaction (NO_2 increases to the original level while ozone decreases). The first two reactions are very fast and the third one is very slow. Therefore, after the flash the concentrations of NO_2 and O_3 will be varied as shown in Figs. 3 and 4 where (1), (2) and (3) refer to the reactions given above. Consequently, if we monitor at an NO_2 absorption line or at an ozone absorption line, we shall obtain a change (a time modulation) of line strength for a considerable length of time after the flash as shown in Figs. 5 and 6 respectively.

Now, if the total flashing energy E and the gain of the monitoring channel are fixed, then the modulated concentration change ($\Delta\rho(NO_2)$ or $\Delta\rho(O_3)$ in Figs. 3 and 4 respectively) or the monitored line strength change ($\Delta I(NO_2)$ or $\Delta I(O_3)$ in Figs. 5 and 6 respectively) will be proportional to the initial concentration of NO_2 in the pollutant sample for the following reason. From the kinetic analysis of reactions (1) and (2), we have

---

†From ref. 42 (Table 44, p. 154)

$$\tau = \frac{1}{k_1[NO]} = \frac{1}{k_1[NO_2]} = 0.1 - 4\ \text{s}$$

for $k_1 = 1.17 \times 10^7\ \text{l mol}^{-1}\ \text{s}^{-1} = 0.5\ \text{ppm}^{-1}\ \text{s}^{-1}$ and $[NO_2] \approx 0.5 - 20$ ppm.

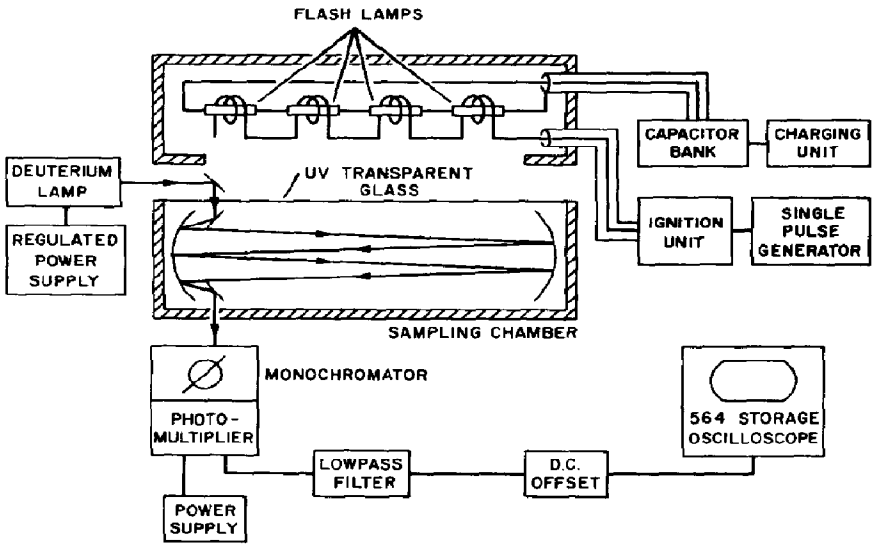

Fig. 7. Schematic diagram of the experimental set-up.

$$\frac{d\rho(NO_2)}{dt} = -kI\rho(NO_2)$$

and

$$\frac{d\rho(NO_2)}{dt} = -\frac{d\rho(O_3)}{dt}$$

The second result is due to the fact that oxygen is abundant in air and every oxygen atom produced by reaction (1) will almost certainly produce an ozone molecule via reaction (2). Integrating these two equations, we have

$$-\Delta\rho(NO_2) \equiv \Delta\rho(O_3) = \{\rho(NO_2)\}_0 (1 - e^{-kE}) \equiv K\{\rho(NO_2)\}_0 \qquad (4)$$

where K is a constant independent of the initial concentration $\{\rho(NO_2)\}_0$, and $E \equiv \int_0^\infty I dt$ is the total flashing energy. All ρs here are expressed in moles per litre and k is the photodissociation reaction constant of reaction (1). Thus by measuring $\Delta I(NO_2)$ or $\Delta I(O_3)$ one obtains a value proportional to the initial concentration of NO_2. The proportionality constant can be determined by calibration. We chose the monitoring wavelength to be at 2550 Å, the strongest ozone line in the whole spectrum, because $\{\alpha(O_3)\}_{2550\,Å} = 3250\ l\ mol^{-1}\ cm^{-1}$ [43], which is 15 - 20 times higher than the two strongest NO_2 lines in the whole spectrum: $\{\alpha(NO_2)\}_{6.3\,\mu m} = 220\ l\ mol^{-1}\ cm^{-1}$ [44], $\{\alpha(NO_2)\}_{4100\,Å} = 170\ l\ mol^{-1}\ cm^{-1}$ [45, 46].

The system we built is schematically shown in Fig. 7. In this figure the light source is a deuterium lamp borrowed from a Beckmann spectrometer. The sampling chamber is a White conjugate-foci folded-path absorption chamber [47, 48]. The flashing system is a series connection of four xenon flash lamps. The capacitor bank and the charging units were built in

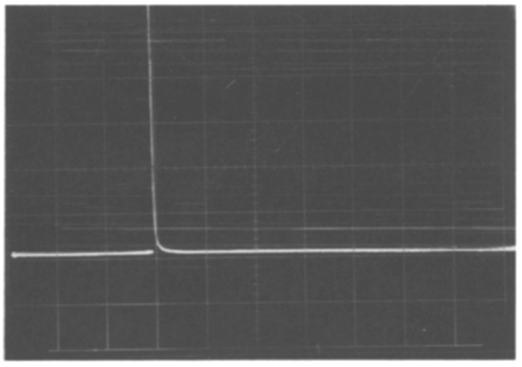

Fig. 8. Output with empty chamber: vertical, 0.05 V per division; horizontal, 1s per division.

this laboratory and can provide a maximum of 6000 J of discharging energy per single flash. The ignition unit provides a medium energy pulse to fire these flash lamps. The single-pulse generator (Data-Pulse 101 Pulse Generator) provides a low energy high peak pulse which is used as the command signal for firing. The UV monochromator is a grating-type Bausch and Lomb 1350 grooves mm^{-1} monochromator. The photomultiplier is an RCA IP28 tube which is quite sensitive in the UV. The low-pass filter is used to filter out the shot noise generated in the photomultiplier, and the d.c. offset circuit is used to offset the large d.c. component in the output such that small a.c. variations can be displayed on the oscilloscope. The operation of this system is as follows.

The sampling chamber is first filled with a known small amount of NO_2 (*e.g.* $\rho(NO_2)$ = 0.5 - 45 ppm). The method of preparing these controlled concentrations is given in Appendix 1. The number of light paths in the sampling chamber is adjusted to eight so that the total absorption length is about $8 \times 35 = 280$ cm. The monochromator is tuned at the maximum ozone absorption line 2550 Å. The flash lamp charging bank is charged to 6000 V and the Tektronix 564 oscilloscope is switched to the manual-triggered slow-sweep storage mode of operation. When the flash lamp is fired, the storage oscilloscope will record permanently the change of intensity of the absorption line. The experimental results are summarized as follows.

When the absorption chamber is empty (*i.e.* filled with normal clean air only), the output monitored at 2550 Å does not show any change in the base line after the flash pulse (Fig. 8), but when the chamber is filled with air containing 0.5 ppm NO_2 the baseline shifts downwards as shown in Fig. 9(a). The baseline shifts downwards more and more after each flash with a faster and faster exponential return when the NO_2 concentration is increased to 1, 2, 5, 10 and 20 ppm as shown in Fig. 9(b) - (f). A plot of the maximum offset amplitudes ($\Delta I(O_3)$ in Fig. 6) of all the above recorded curves *versus* $\rho(NO_2)$ shows an approximately straight line variation as shown in Fig. 10. This verifies the calculation given by eqn. (4). It is exactly this linear property that makes proportional measurements on low concentrations of NO_2

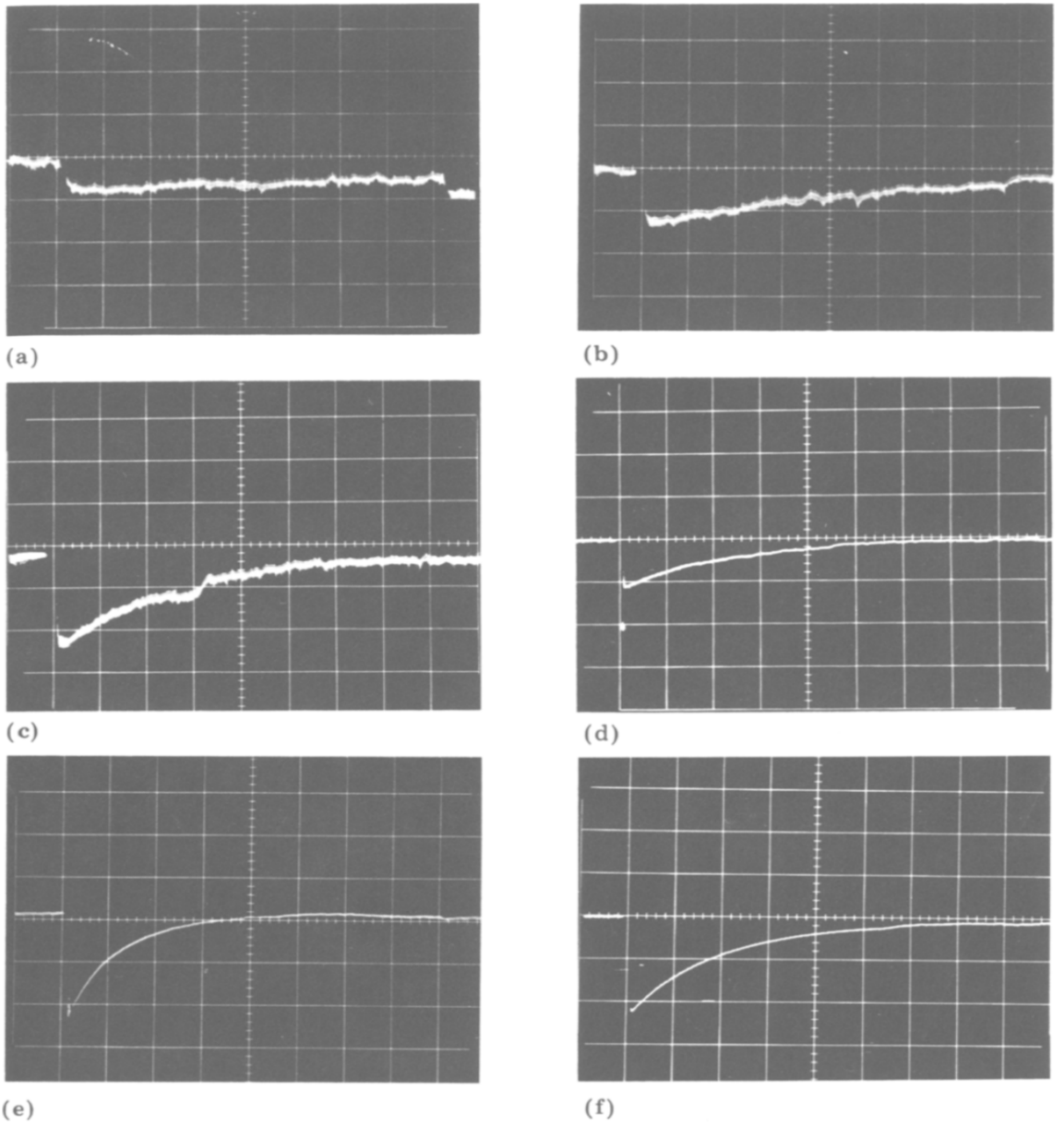

Fig. 9. Output with (a) 0.5 ppm NO_2, (b) 1 ppm NO_2, (c) 2 ppm NO_2, (d) 5 ppm NO_2, (e) 10 ppm NO_2, (f) 20 ppm NO_2: (a), (b), (c) vertical 0.02 V per division, horizontal 5 s per division; (d), (e) vertical 0.05 V per division, horizontal 5 s per division; (f) vertical 0.1 V per division, horizontal 1 s per division.

possible. A plot of the rise time† τ of the offset curves *versus* $\rho(NO_2)$ can be approximated by a hyperbolic curve $\tau\rho(NO_2)$ = const. as shown in Fig. 11. This relation can also be predicted theoretically from a kinetic analysis of

†The rise time is defined as the time between the maximum offset point and one-third of the maximum offset point in all the recorded curves.

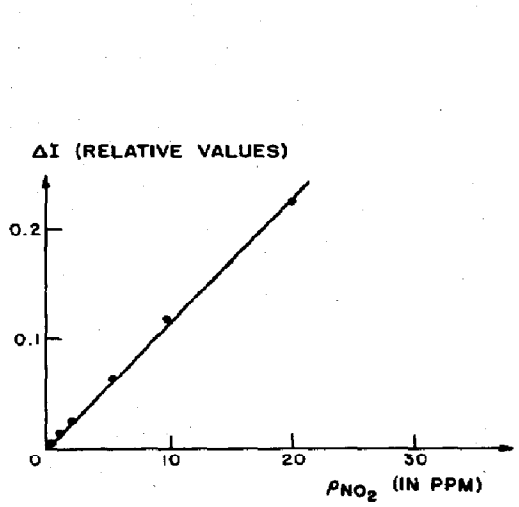

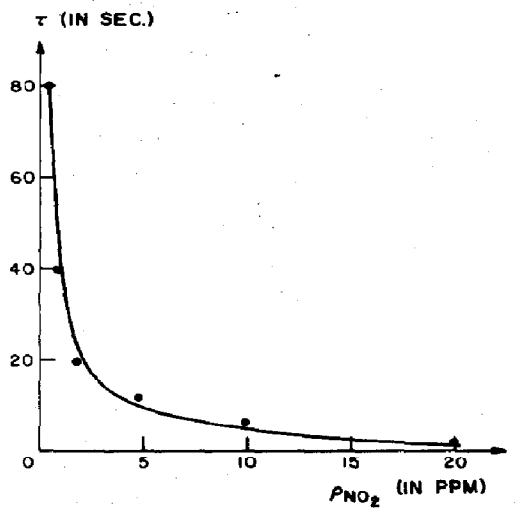

Fig. 10. Linearity of concentration modulation: ●, data measured from photographs (Figs. 8 and 9).

Fig. 11. Lifetime *vs.* concentration relation in concentration modulation: ●, experimental data measured from Figs. 8 and 9; the solid curve represents the theoretical relation, $\tau = 50/\rho(NO_2)$.

reactions (1) - (3) (Appendix 2). The reproducibility of the above results is about 90% if the position of the light source, the position of the monochromator and the voltage supply of the photomultiplier are fixed. Actually we can produce exactly the same curve with a consecutive flash.

However, when we shift the monitoring wavelength to 4100 Å, the strongest NO_2 line in the visible, the result is much less sensitive than that described above. When the chamber is empty and the low-pass circuit is off, the noise is very high as shown in Fig. 12(a). This makes it very difficult to detect the spectroscopic line variation of NO_2 without concentration modulation. Even when the filtering circuit is connected, the low frequency noise (Fig. 12(b)) still makes detection impossible. Also, the average baseline drifts with respect to time. When the chamber is filled with air containing 5 ppm NO_2, the baseline does not show any significant change after the flash pulse (Fig. 12(c)). A measurable shift upwards (Fig. 12(d)) is observed only when the chamber is filled with air containing 10 ppm (or more) NO_2. The modulated change of line intensity is seen to be very noisy and the reproducibility is only about 60%.

It is seen from these experimental results that the detection of NO_2 by monitoring at the 2550 Å ozone line is linear, sensitive and reproducible. The minimum detectable concentration of NO_2 from this method is 0.5 ppm which is difficult to reach using conventional spectroscopic techniques with the same path length. The reason for this increase of sensitivity is twofold: (1) the absorption at the 2550 Å ozone line is much stronger than that at any NO_2 line; (2) the optical noise (in this case, the optical noise is mostly

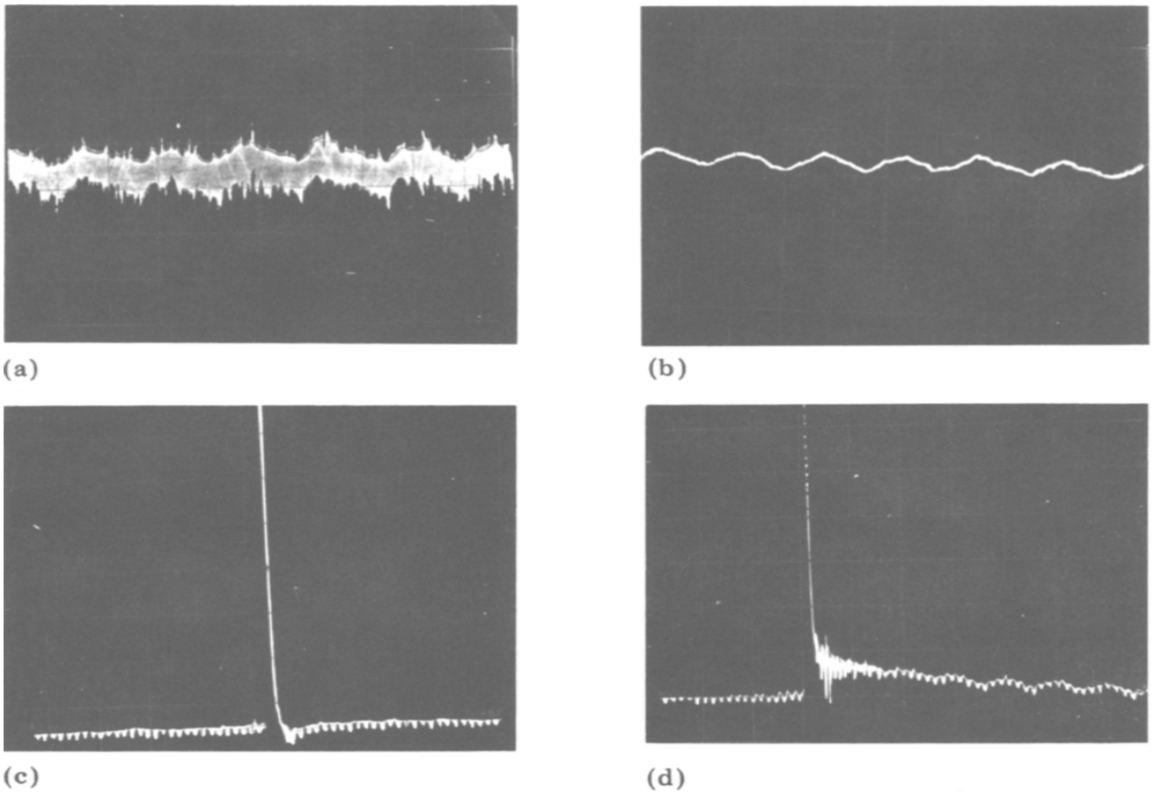

Fig. 12. Output at (a) 4100 Å, empty chamber, without low-pass filter, (b) 4100 Å, empty chamber, with low-pass filter, (c) 4100 Å, 5 ppm NO_2, (d) 4100 Å, 10 ppm NO_2; (a), (b) vertical 0.01 V per division, horizontal 20 ms per division; (c), (d) vertical 0.03 V per division, horizontal 0.3 s per division.

d.c. drift and a.c. low frequency noise as shown in Fig. 12(b)) will not affect the measurements as explained in Section 3.1.

Consequently, it is seen that the advantage of shifting the detection to a high absorption low noise region by concentration modulation is verified experimentally for the case of detecting NO_2 in air.

5. Signal processing applied to concentration modulation†

If a continuously pulsed UV beam is applied to a polluted air sample with the apparatus shown in Fig. 13, then the concentration of, say, NO_2 in the sampled air will look like that shown in Fig. 14(a) and the monitored output V_{out} (if the monochromator is tuned at a characteristic absorption line of NO_2) will look like that shown in Fig. 14(b). Now if we use an

† A good background review for the signal processing technique discussed here can be found in ref. 50.

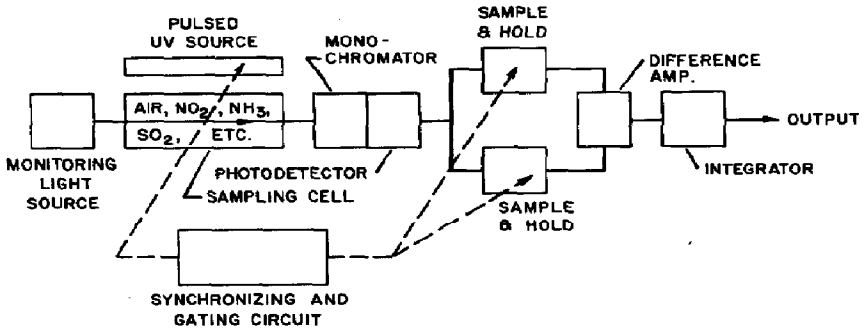

Fig. 13. A signal-processing system for detecting continuously concentration modulated signals.

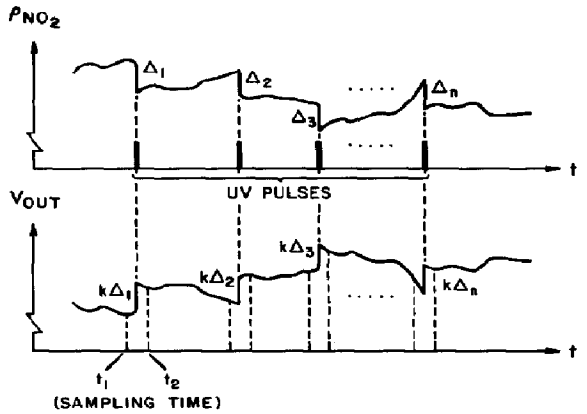

Fig. 14. (a) Continuous step modulation of NO_2 concentration; (b) monitored output of the continuous step modulation.

electronic gating technique to sample the output voltage just before and just after each UV pulse as shown in Fig. 14(b) and feed the sampled results into a difference amplifier (Fig. 13), then the accumulated output after the integrator will be proportional to $\Sigma\Delta_i \equiv \Delta_1 + \Delta_2 + \ldots + \Delta_n$. This output is, in turn, proportional to the original concentration of NO_2 in the air sample averaged over space and time because each Δ_i is proportional to the concentration of NO_2 at the pulsing time (see eqn. (4) of Section 4). Optical noise will be effectively suppressed in this scheme as can be seen from the following explanation.

(1) Line-overlapping noise: since the UV pulses do not dissociate any major atmospheric molecules because they are not photosensitive at the dissociation wavelengths of the pollutants, the line-overlapping effect will be cancelled out after the difference amplifier (Fig. 13).

(2) Background radiation noise: this will also be cancelled out after the difference amplifier because it is not affected by the UV modulation.

(3) D.c. fluctuation noise: again, for the same reason, this noise will be cancelled out at the output if the sampling times t_1 and t_2 (Fig. 14(b)) are closely located around each UV pulse.

This system of using a sample–difference–integration method is different from the conventional signal-averaging system. The latter changes the analogue signal in each cycle into digital form (by means of sampling and analogue-to-digital conversion) and stores it cumulatively in a digital memory such that the signal is cumulatively summed while the random noises are averaged out. Strictly speaking, these noises will not be completely averaged out. Instead, in the summed output the noise amplitude (or standard deviation of the noise) will be proportional to $n^{1/2}$ where n is the number of cycles summed. (Here, we assume that the noise at each corresponding point in each cycle has a normal probability distribution and that these noises are statistically independent from cycle to cycle.) The signal amplitude at the output is, however, proportional to n because of the repetitive nature of the signal in each cycle. Therefore the signal-to-noise ratio for the conventional signal-averaging scheme should be proportional to $n/n^{1/2}$ or $n^{1/2}$. In contrast, in the scheme shown in Fig. 14(b), the low frequency optical noises immediately before and immediately after each flashing pulse are not completely independent of each other. They have significant correlative variations if the sampling times t_1 and t_2 are close to each other and if the high frequency electronic noise is already filtered out by a low-pass filter as was the case in our experiments (Fig. 7). Therefore, when one of these correlated noises is subtracted from another by the difference amplifier shown in Fig. 13, the output noise for each single cycle alone should already be able to cancel out. Thus the n-cycle summed noise after the difference amplifier–integrator stage should be much lower than that in the conventional signal-averaging scheme. Consequently the signal-to-noise ratio in the scheme discussed here should be much higher than that in the conventional signal-averaging scheme if the same number of cycles is summed.

The above scheme (Figs. 13 and 14) is one possible scheme for detecting the step-modulated signals from noise. With proper modifications, recent developments on matched filters and linear predictive filtering etc. may also be applicable to the sensitive detection of these step signals. Currently we are working on experiments using this second scheme. We expect the experimental results to be published as a subsequent paper in the near future.

6. Conclusion

It is seen that the main idea of concentration modulation is to create some controlled difference between the signal (or the characteristic line intensity of the pollutant) and the optical noise such that we can either shift the detection to a high absorption low noise region or use some signal-processing technique to detect this weak but modulated signal from the unmodulated noise. Our experiments on the first approach show that the

concept is a practical one and that it increases significantly the sensitivity of detection. Other characteristics of this system are that it can be used to measure various photochemical pollutants when the monitored wavelength is changed accordingly. It is a fast detection process and does not require a high resolution monochromator or an elaborate chemical process for purifying the air samples.

Acknowledgments

The author wishes to acknowledge the following institute and persons with deep appreciation: the National Science Foundation for their financial support; Jay H. Harris for his scientific judgement and encouragement; Frank S. Barnes for his administrative management and discussions; Vernon Derr and Steward Strickler for their technical suggestions; Carl T. Johnk for his careful reading of the English of the original manuscript.

References

1 G. Porter and M. A. West, Flash photolysis, In G. G. Hammes (ed.), Investigation of Rates and Mechanisms of Reactions, Part II (3rd edn.), Wiley, New York, 1974, pp. 367 - 462.
2 L. I. Grossweiner, A. G. Kaluskar and J. F. Baugher, Int. J. Radiat. Biol., 29 (1976) 1 - 16.
3 J. Baugher, L. Grossweiner and J. Y. Lee, Photochem. Photobiol., 25 (1977) 305 - 306.
4 S. Classon and C. M. Backman, Chem. Scr., 10 (1976) 143 - 144.
5 K. H. Knauer and R. Gleiter, Angew. Chem., 89 (1977) 116 - 117.
6 R. Kuhlmann and W. Schnabel, Angew. Makromol. Chem., 57 (1977) 195 - 210.
7 G. Porter, Proc. R. Soc. London, Ser. A, 200 (1950) 284.
8 M. Green and G. Tollin, Rev. Sci. Instrum., 38 (1967) 1316 - 1321.
9 B. Ke, R. W. Treharne and C. McKibben, Rev. Sci. Instrum., 35 (1964) 296 - 300.
10 J. A. Burt, Anal. Chem., 49 (1977) 1130 - 1134.
11 H. S. Johnston, G. E. McGraw, T. T. Paukert, I. W. Richards and J. V. D. Bogaerde, Proc. Natl. Acad. Sci. U.S.A., 57 (1967) 1146 - 1153.
12 A. C. Stern, Air Pollution, Vol. III (3rd edn.), Academic Press, New York, 1976.
13 E. R. Stephens, P. L. Haust, R. C. Doerr and W. E. Scott, Ind. Eng. Chem., 48 (1956) 149B.
14 R. Stair *et al.*, Ozone chemistry and technology, Adv. Chem. Ser., 21 (1959) 269 - 285.
15 P. L. Haust, Appl. Spectrosc., 24 (1970) 161 - 174.
16 K. W. Kothe, U. Brinkmann and H. Walther, VDI Ber. (Ver. Dtsch. Ing.), 247 (1974) 28 - 32.
M. Bass, T. F. Deutsch and M. J. Weber, in A. K. Levine and A. T. DeMaria (eds.), Laser, Vol. 3, Dekker, New York, 1971.
17 H. D. Axelrod, J. H. Cary, J. E. Bonelli and J. P. Lodge, Jr., Anal. Chem., 41 (1969) 1956.
18 T. R. Andrew and P. N. R. Nicols, Analyst (London), 90 (1970) 367.
19 J. A. Gebwach, M. Bimbaum, A. W. Tucker and C. L. Fincher, Opto-electronics, 4 (1972) 155.

20 D. Neuberger and A. B. F. Duncan, J. Chem. Phys., 22 (1954) 1693.
21 G. D. Hickman and R. B. Moore, Proc. 13th Conf. on Great Lakes Research, Buffalo, N. Y., 1970.
22 R. K. Stevens, A. E. O'Keefe, J. D. Mulik and K. J. Krost, Anal. Chem., 43 (1971) 827.
23 D. G. Greer and T. J. Bydalek, Environ. Sci. Technol., 7 (1973) 153.
24 V. H. Regener, J. Geophys. Res., 69 (1964) 3795 - 3800.
25 A. Fontijn, A. Sataldel and A. R. J. Conco, Anal. Chem., 45 (1970) 575.
26 A. Alford, Biomed. Mass Spectrom., 4 (1977) 1 - 22.
27 R. T. Menzies, Appl. Phys. Lett., 22 (1973) 592.
28 R. T. Menzies, Opto-electronics, 4 (1973) 179.
29 V. E. Den and C. G. Little, Appl. Opt., 9 (1970) 1976.
30 H. Kildal and R. Byer, Proc. IEEE, 59 (1971) 1644.
31 M. C. Fowler and P. J. Berger, EPA Rep. 650/2-74-020, United States Environmental Protection Agency, Research Triangle, North Carolina, 1974.
32 M. P. McCormick and W. H. Fuller, Jr., AIAA J., 11 (1973) 244.
33 W. J. Hurley, J. Chem. Educ., 43 (1966) 236 - 240.
34 M. J. D. Low, J. Chem. Educ., 43 (1966) 637 - 643.
35 M. J. D. Low and F. D. Clancy, Environ. Sci. Technol., 1 (1967) 73 - 74.
36 D. Onderdelinder and L. Strackee, Rev. Sci. Instrum., 48 (1977) 752.
37 U. Bonafe, G, Cesari, G. Giovanelli, T. Tirabassi and D. Vittori, Atmos. Environ., 10 (1976) 469 - 474.
38 H. Goldstein, M. Bortaer, R. Grenda, R. Dick and A. R. Barringer, Can. J. Remote Sensing, 2 (1976) 30 - 41.
39 H. Ford and H. Gordon, J. Chem. Phys., 27 (1957) 1156, 1277.
40 H. Ford, An experimental study of oxidants and organics in urban atmospheres, Tech. Reps. nos. XI, XII, XIII, Project S-1388, Stanford Research Institute, 1956.
41 H. Johnston and H. Crosby, J. Chem. Phys., 22 (1954) 689.
42 P. A. Leighton, Photochemistry of Air Pollution, Academic Press, New York, 1961.
43 J. G. Calvert and J. N. Pitts, Photochemistry, Wiley, New York, 1966.
44 V. E. Derr, Memorandum to National Air Pollution Control Administration, August 15, 1969, Fig. 6 - 1.
45 T. C. Hall and F. E. Blacet, J. Chem. Phys., 20 (1952) 1745.
46 J. K. Dixon, J. Chem. Phys., 8 (1940) 157.
47 J. V. White, J. Opt. Soc. Am., 32 (1942) 285.
48 H. Bernstein and G. Herzberg, J. Chem. Phys., 16 (1948) 30.
49 D. Middleton, Introduction to Statistical Communication Theory, McGraw-Hill, New York, 1960 (analogue signal processing).
L. R. Rabiner and C. M. Rader, Digital Signal Processing, IEEE Press, New York, 1972 (digital signal processing).

Appendix 1. Method of preparing a polluted air sample with a known NO_2 concentration.

The NO_2 gas is produced by adding HNO_3 to copper powder and sealing it in the vessel shown in Fig. A1. The pressure inside the cell is much higher than the atmospheric pressure outside. Now if the switch is opened for about a second a mixture of NO_2 and N_2O_4 gases will flow into and fill up the polyethylene tube. A syringe with a needle can then be used to extract any desired volume of the mixed gas from this polyethylene chamber. This mixture should be at a pressure very close to atmospheric pressure, because otherwise the gas will escape from the needle in order to

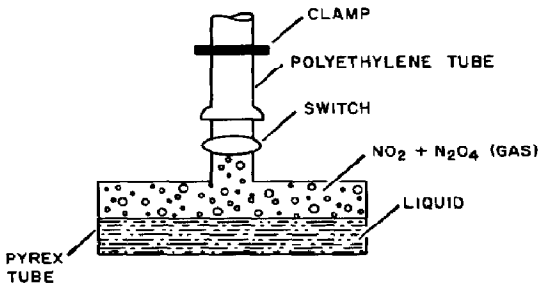

Fig. A1. Sample preparation device.

balance the pressure. This known volume of gas at atmospheric pressure is actually a mixture of N_2O_4 and NO_2. If one injects this mixture into the long-path absorption chamber which contains nothing but normal air, all the N_2O_4 will decompose into NO_2 owing to the dilution effect. The amount of NO_2 in the absorption chamber can be calculated from the volume of the mixture in the syringe before injection in the following manner.

N_2O_4 and NO_2 are in chemical equilibrium in the syringe

$$\begin{matrix} C_1 & & C_2 \\ N_2O_4 & \underset{k_2}{\overset{k_1}{\rightleftharpoons}} & 2NO_2 \end{matrix}$$

where C_1 and C_2 (expressed in atmospheres) are the concentrations of N_2O_4 and NO_2 respectively before the injection and k_1 and k_2 are the reaction constants. At equilibrium we have

$$k_1C_1 = k_2C_2^2 \tag{A1}$$

Also, because the total pressure in the syringe is 1 atm, we have

$$C_1 + C_2 = 1 \tag{A2}$$

For n cm^3 of mixture at 1 atm pressure in the syringe, the total number of moles of NO_2, if the N_2O_4 is fully decomposed, is $(2C_1k + C_2k)n$ mol where $k \equiv (2.24 \times 10^4)^{-1}$ mol cm^{-3} atm^{-1} is the factor use to convert moles per cubic centimetre into atmospheres. Therefore, the volume of NO_2 in cubic centimetres after injection into the absorption chamber is $(2C_1k + C_2k)n/k \equiv n(2C_1 + C_2)$ cm^3. Consequently, the concentration of NO_2 (in parts per million by volume) in the large absorption chamber is

$$\rho(NO_2) = \frac{(2C_1 + C_2)n}{V} \times 10^6 \text{ ppm} \tag{A3}$$

where V is the total volume of the absorption chamber in cubic centimetres. Eliminating C_1 and C_2 from eqns. (A1), (A2) and (A3) with $k_1/k_2 = 0.1426$ atm at 25 °C [A1] and $V = 2.35 \times 10^6$ cm^3 we have

$$\rho(NO_2) = 0.5n \text{ ppm}$$

i.e. drawing n cm^3 of mixture gas from the polyethylene tube and injecting it into the sealed absorption chamber results in a polluted air sample in the chamber with a known NO_2 concentration of $0.5n$ ppm.

Reference to Appendix 1

A1 F. Verhook and F. Daniels, J. Am. Chem. Soc., 53 (1937) 1250.

Appendix 2. Relation between the NO_2 concentration and the signal decay time

Theoretically, the recovery time after flash modulation can be determined from reaction (3) of Section 4:

$$O_3 + NO \xrightarrow[k_3]{} NO_2 + O_2$$

In this reaction the annihilation rate of ozone is

$$\frac{d\rho(O_3)}{dt} = -k_3\rho(O_3)\rho(NO)$$

Here, $\rho(O_3)$ and $\rho(NO)$ after the flash should be equal in our simulated air sample because they are negligible before the flash and they are produced in equal amounts after the flash by reactions (1) and (2). Therefore, integrating the above equation with $\rho(O_3) = \rho(NO)$ we have

$$\frac{1}{\rho(O_3)} = k_3 t + \frac{1}{\Delta\rho(O_3)}$$

where $\Delta\rho(O_3)$ is the maximum offset concentration of ozone immediately after the flash. Let the decay time τ be defined as the time for $\rho(O_3)$ to reach one-third of its maximum offset value; then the last equation becomes

$$3 = k_3\tau\Delta\rho(O_3) + 1$$

or

$$\tau\Delta\rho(O_3) = 2/k_3$$

Therefore, through eqn. (4) of Section 4, we have

$$\tau\{\rho(NO_2)\}_0 = \text{constant}$$

This relation is experimentally checked as shown in Fig. 11.